Thermal conductivity and Raman spectra of carbon fibers

J. Heremans
General Motors Research Laboratories, Warren, Michigan 48090-9055

I. Rahim and M. S. Dresselhaus
Department of Electrical Engineering and Center for Materials Science and Engineering, Massachusetts Institute of Technology, Cambridge, Massachusetts 02139

(Received 11 June 1985)

The thermal conductivity between 12 and 300 K is reported for graphite fibers carbonized from a variety of precursors, including spun polyacrylonitrile, petroleum pitch, or grown by chemical vapor deposition of methane. The fibers were studied as grown as well as heat treated to temperatures up to 3000 °C. First-order Raman spectra of the same fibers were taken with use of a microprobe, and the intensity ratio I_{1360}/I_{1580} between the disorder-induced line at 1360 cm^{-1} and the Raman-allowed line at 1580 cm^{-1} correlates well with the amplitude of the low-temperature thermal-conductivity data. Using the Kelly model for the phonon-dominated thermal conductivity, we deduce the defect-limited phonon mean free path L_ϕ from our data below 100 K. We find L_ϕ approximately equal to L_a, the x-ray in-plane correlation length which had been related by Tuinstra and Koenig to the Raman intensity ratio I_{1360}/I_{1580}. We show further correlations between L_ϕ and the electrical resistivity ρ, the interplane distance $\frac{1}{2}c_0$, and the c-axis correlation length L_c.

INTRODUCTION

Recently published[1,2] values of the thermal conductivity of fibers grown by carbon chemical vapor deposition and subsequently heat treated to 3000 °C show that these readily available materials can conduct heat at least four times better than copper near room temperature. The present study is aimed at characterizing graphite fibers prepared in different ways by thermal conductivity measurements along the filament axis. The thermal conductivity is further related to other measured quantities known to characterize the degree of disorder in the material, such as x-ray diffraction[3] or Raman spectroscopy.[3,4]

The majority of carbon or graphite fibers are obtained in either of three ways.

(1) Carbonization of spun polyacrylonitrile ("PAN-based" fibers).

(2) Carbonization of spun petroleum pitch ("pitch-based" fibers).

(3) Carbon chemical vapor deposition, mainly from benzene or methane.

In this paper, we first review the scanty data available for the longitudinal thermal conductivity K of various types of graphite fibers. Then we report a systematic series of measurements of K, made between 10 and 300 K, on fibers of different origin and prepared under a variety of heat-treatment temperatures chosen. Our samples are chosen as prepared or heat treated so as to bracket the possible range of conductivities achievable with each type of fiber.

Finally we report first-order spectra taken with a Raman microprobe on individual fibers taken from the same batches that were used for thermal conductivity measurements. Obvious experimental correlations can then be established between the phonon mean free path, the intensity of the disorder-induced Raman peak at 1360 cm^{-1}, the c-axis lattice spacing, and the electrical conductivity. Carbon fibers grown by carbon chemical vapor deposition are highly graphitizable.

It was pointed out for benzene-derived[1] and methane-derived[2] fibers, even as early as 1958,[5] that the longitudinal thermal conductivity K of vapor-grown fibers heat treated around 3000 °C is comparable to that of single-crystal graphite. Most recently it has been shown[2] that heat treatment of the fibers to 3000 °C increases the room-temperature thermal conductivity of as-grown methane-derived fibers from 40 to ~ 2000 $W\,m^{-1}\,K^{-1}$.

Data for pitch-based fibers are relatively sparse. The most reliable data are reported on Union Carbide[6] type-VSC-25 fibers in Ref. 7. The room-temperature value of K is 500 $W\,m^{-1}\,K^{-1}$.

A summary of the data available in the literature for the thermal conductivity of PAN-based fibers is given in Fig. 1. The data were either obtained using bundles of fibers, or deduced from measurements on composite materials. Radcliffe and Rosenberg[8] measured bundles of Courtaulds Ltd. general purpose (A), high-tensile (HT), and high-modulus (HM) fibers: see the data points in Fig. 1. These extrapolate well, at $T > 100$ K, into the data obtained by Pilling and co-workers[9] on Morganite Modmore high modulus (HMS, line 1 in Fig. 1) and high-tensile strength (HTS, line 2) fibers, though the latter results were deduced from measurements on composites. Earlier measurements obtained on fiber bundles are reported on PAN-based fibers[10] heat treated at different temperatures (lines 3, 4, and 5 of Fig. 1). Finally the data of Hull *et al.*,[11] obtained on composites in the temperature range of 375 to 625 K on Stackpole Panex 30 Y/800 d and Celanese Celion DG 125 fibers are also reported (lines 6

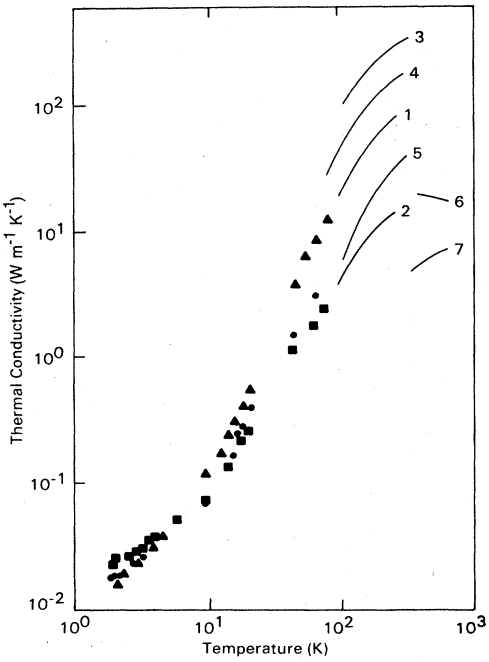

FIG. 1. Thermal conductivity of PAN-based fibers. The data points are taken from Ref. 8: △ for the HM type, ● for the HT type, ■ for the A type. The solid lines represent the thermal-conductivity data measured by Refs. 9—11. Lines 1 and 2 are data from Ref. 9, 1 for HMS-type fiber, 2 for HTS. Lines 3, 4, and 5 are from Ref. 10, for fibers heat treated at 2800, 2600, and 1400 °C, respectively. Lines 6 and 7 are copied from Ref. 11, for Panex 30 Y/800 d and Celion DG 125, respectively.

and 7), despite the surprising temperature dependence observed in line 6. The picture that emerges is unclear. It is probable that some data reported above 100 K, where radiative heat losses become an important source of experimental error, are not entirely reliable.

EXPERIMENTAL RESULTS AND DISCUSSION

The fibers used in this work are:

(i) Vapor-grown fibers[12] deposited from natural gas around 1100 °C, and similar fibers heat treated to 3000 °C.

(ii) Commercially available pitch-based fibers: Union Carbide,[6] type P 100 grade VSO 054 and type P 55 grade VSB-16-OS, which were heat treated by the manufacturer. The fibers used in this work were unsized (not coated).

(iii) PAN-based fibers C 6000 from Celanese,[13] also unsized, and the same fibers heat treated to 3000 °C.

(iv) A highly stretched PAN-based fiber, supplied by Fibers Materials, Inc. (FMI) (Ref. 14).

We characterized our samples by x-ray diffraction, deducing the interplane distance from the ⟨002⟩ peak and the c-axis correlation length L_c from its broadening.[15] The data are summarized in Table I. The room-temperature resistivity was measured on several filaments of each bundle used to measure the thermal conductivity. Resistivity measurements employed a four-probe method and the geometrical factors were measured in an optical microscope or in a scanning electron microscope. The values are reported in Table I and are accurate to within 15%—which is the scatter in data from filament to filament for all types of fibers except those supplied by Fibers Materials Inc.: in a bundle of these, a few filaments have a resistivity three times smaller than the average. A bun-

TABLE I. Properties of the samples for the chemically vapor-deposited (CVD), pitch-based (P 55 and P 100), and PAN-based (FMI, C 6000) fibers. We report in row 1 the highest temperature to which the fibers have been exposed in our laboratory. The x-ray data $d_{\langle 002\rangle}$ and L_c, the room-temperature resistivity ρ(RT) and thermal conductivity K(RT), and the tensile strength and modulus are reported: (a) as measured by us on the sample used for the thermal conductivity studies and (b) as reported by the manufacturers. The phonon mean free path L_ϕ, and the ratio of intensities of Raman scattering at 1360 cm^{-1} to that at 1580 cm^{-1} as deduced from the present measurements are summarized. The last six rows report the values for the parameters [peak position, intensity, and line width half-width at half maximum (HWHM)] obtained by fitting Lorentzian line shapes to the Raman peaks.

Property	Units	CVD	CVD HT	P 55	P 100	C 6000	C 6000 HT	FMI
Heat-treat. temp.	°C	1130	3000				3000	
$d_{\langle 002\rangle}$	nm	0.347	0.335	0.341	0.337	0.353	0.3395	0.341
L_c	nm	3.8	≥ 100	8	18	1.6	7.2	5.4
ρ(RT) (a)	Ω m	1.02×10^{-5}	7.1×10^{-7}	9.6×10^{-6}	3.6×10^{-6}	1.8×10^{-5}	5.9×10^{-6}	3.0×10^{-6}
(b)				7.5×10^{-6}	2.5×10^{-6}	1.5×10^{-5}		
K(RT) (a)	W m^{-1} K^{-1}	35	1950	100	300	12	155	140
(b)				100	520			
Strength (b)	G Pa			2.1	2.2	2.7		3.3
Modulus (b)	G Pa			380	720	230		480
L_ϕ	m	3.6×10^{-9}	2.9×10^{-6}	1.5×10^{-8}	1.3×10^{-7}		2.8×10^{-8}	2.2×10^{-8}
I_{1360}/I_{1580}		0.778	0	0.316	0.109		0.196	0.337
Peak position	cm^{-1}	1605	1582	1572	1569		1570	1575
Intensity	arb. units	24 400	3900	4000	13 800		7000	12400
Width	cm^{-1}	26.5	6.8	16	10.5		10	11
Peak position	cm^{-1}	1379		1350	1352		1350	1350
Intensity	arb. units	17 700		480	450		1700	5400
Width	cm^{-1}	26		17	20		20	20

dle of each type of fiber was then mounted in the cryostat, and the geometrical ratio of the bundle was now deduced from its electrical resistance and the previously measured resistivity. The thermal and electrical geometrical ratios are assumed equal. The thermal conductivity measurement technique is described elsewhere.[2] The temperature dependence of the electrical resistivity of the various fibers is shown in Fig. 2, and in Fig. 3 we report the temperature dependence of the thermal conductivity of the same fibers.

Since in all the fibers studied the graphite-layer planes are preferentially oriented along the fiber axis,[16–18] we can reasonably assume that we are measuring the in-plane thermal conductivity of graphites or carbons of varying degrees of ordering, except perhaps in the case of Celion 6000. At temperatures above 10 K, heat is transported along the graphite planes almost entirely by phonons. The theory for the thermal conductivity in the case where defects limit the phonon mean free path was developed by Kelly.[19] We follow here the same treatment as in Ref. 2: we assume that the phonon dispersion relations are little affected by the degree of order, a hypothesis which is consistent with the similar temperature dependence of our data in Fig. 3 below 100 K, and with the persistence of the 1580 cm^{-1} Raman line, as we shall discuss later. The effect of disorder on the phonon dispersion relations was considered from a theoretical point of view in Ref. 4.

Kelly's[19] theory essentially describes the thermal conductivity as

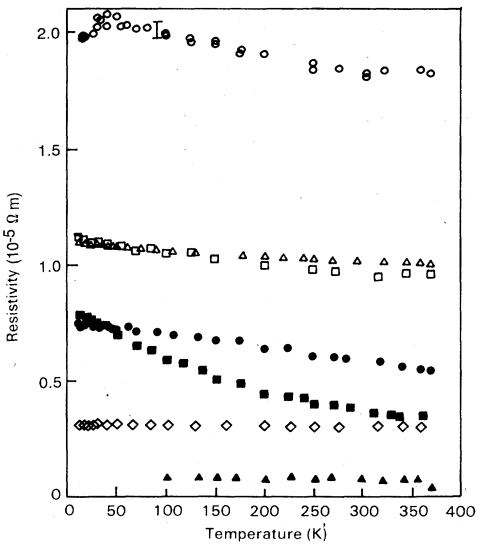

FIG. 2. Temperature dependence of the electrical resistivity of the various fibers, using the following legend: C 6000 (○), as-grown CVD (△), P 55 (□), C 6000 heat treated at 3000 °C (●), P 100 (■), FMI (◇), and CVD fiber heat treated at 3000 °C (▲). An estimate of the absolute error (see error bar) in the data points is provided by the results for C 6000: two different sets of samples were measured and the data were superimposed without any normalization. C 6000 is an abbreviation for Celion 6000.

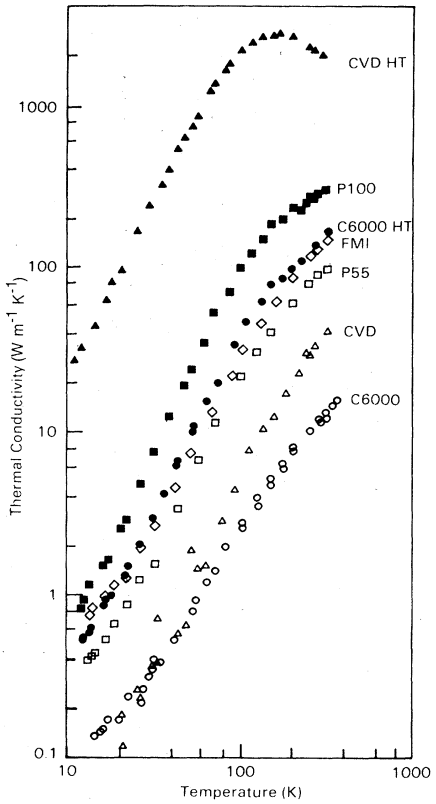

FIG. 3. Temperature dependence of the thermal conductivity of carbon and graphite fibers. From top to bottom (at 300 K) we identify the data for each of the fibers as follows: The CVD fibers heat treated at 3000 °C (▲), P 100 (■), the C 6000 heat treated at 3000 °C (●), the FMI fiber (◇), P 55 (□), the as-grown CVD fibers (△), and C 6000 (○). For C 6000 again two bundles were measured.

$$K = L_\phi \sum_p \int_\sigma S(\sigma,p) v(p) d\sigma \,, \tag{1}$$

where S is the heat capacity, v is the velocity of a phonon in a mode p, and σ is the normalized wave vector, the integral being performed over the whole Brillouin zone. Three phonon modes p have to be considered, in-plane longitudinal and transverse and out-of-plane transverse, with the propagation direction in the the plane. L_ϕ is the phonon mean free path, which is assumed to be independent of temperature, phonon mode, or wave vector in the present picture. This approximation is acceptable when phonon scattering by defects is dominant. We estimated the complete integral numerically, and if we assume that the elastic constant $C_{44}=0$, this theory essentially predicts a $T^{2.3}$ law for temperatures above 30 K and below the temperature where phonon-phonon umklapp processes become dominant. As this is the case for most of our experimental curves, though not for Celion 6000, we can quantitatively fit each of them to Eq. (1) using only one adjustable parameter L_ϕ. The values of the phonon mean free path L_ϕ so obtained are reported in Table I. The thermal-conductivity results on Celion 6000 are unusual in two aspects. Unlike the case of other fibers,

the temperature exponent between 30 and 300 K is lower than 2.3. Below 25 K, the exponent is further lowered down to 1. A similar behavior was observed by Radcliffe and Rosenberg[8] also on PAN-based fibers, although their curves show a transition at a lower temperature. Obviously data much below 10 K must be gathered before any quantitative conclusions can be reached. It is nevertheless worth pointing out that PAN-based fibers contain ribbon-like features[18,20] with "ribbons" made by stacking 5—10 graphite layers. A transverse out-of-plane phonon propagates along the plane at a velocity of approximately 1000 m sec^{-1} (see elastic constants in Ref. 19). Phonons with an energy of 25 K (where the kink in temperature-dependent thermal conductivity occurs) have a wavelength of roughly 20 Å, i.e., a typical thickness for a ribbon.[20] We thus concur with Ref. 8 and attribute the change in the temperature dependence of the thermal conductivity to a size effect.

We used a Raman microprobe, which could illuminate an area as small as 4×4 μm, to obtain the first-order spectra of individual filaments of the same batch as those used for the thermal and electrical conductivity measurements. At the argon-ion laser wavelength, 4880 Å, the optical skin depth of the fiber is $\sim$600 Å. The frequency shift was measured with a double grating monochromator, a diode array detector, and a multichannel analyzer. The quality of the data nevertheless depended on the reflectivity of the fibers studied. The PAN-based fibers, in particular Celion 6000, both in its as received and heat-treated forms, had a rather rough surface at the laser wavelength, thus severely restricting the accuracy of our Raman microprobe data. The FMI fibers had smoother surfaces, but their diameters (4 μm) were close to the minimum size of the focused laser beam. This also affected the quality of the spectra. Although the FMI fibers we used were not specifically uncoated, as were all other fibers, we expect that the laser beam evaporated the sizing layer during our Raman experiment.

The Raman spectrum of disordered carbons and carbon fibers has been previously discussed in detail.[3,4,21] It has been used to provide important information on the crystalline perfection. Indeed, while in "perfect" graphite, the only allowed high-frequency Raman line (at $\sim$1580 cm^{-1}) is limited to the Brillouin-zone-center mode, the selection rules are relaxed in disordered graphite systems. Thus, for less perfect graphites, contributions to the Raman spectrum are observed at phonon frequencies where there is a maximum in the phonon density of states, even though these phonons are not zone-center phonons. This effect gives rise to the $\sim$1360 cm^{-1} line studied here. We therefore consider as a measure of "disorder" the ratio of the intensities of the disorder induced to Raman allowed lines: I_{1360}/I_{1580}. This ratio is zero in perfect graphites, and can reach values as high as 1.2 in some amorphous carbons. We fitted our Raman spectra (see Fig. 4) to Lorentzian line shapes. The parameters of these fits (position, amplitude above background, and line width) are reported in Table I, along with the ratio of integrated intensities I_{1360}/I_{1580}. In Fig. 5, we plot this intensity ratio as a function of the phonon mean free path L_ϕ which was obtained from the low-temperature thermal conductivity

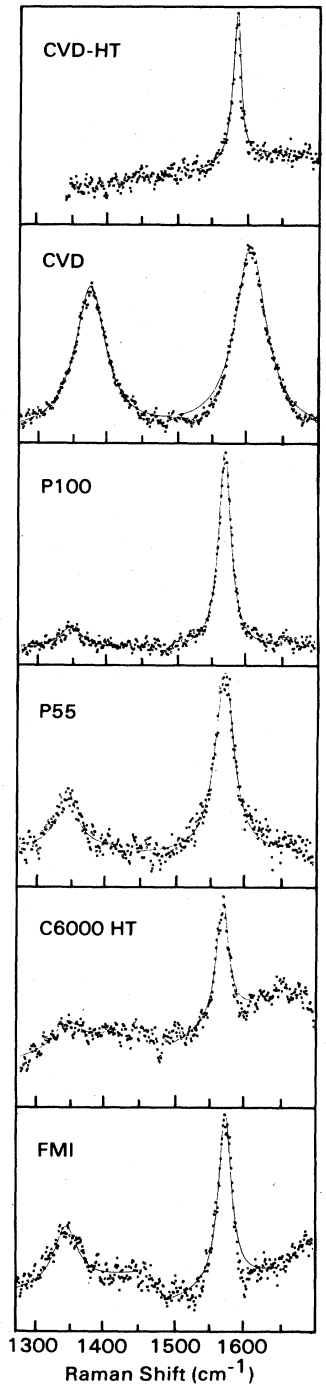

FIG. 4. First-order Raman spectra for the fibers studied here. CVD fibers heat treated at 3000°C show only the Raman-allowed line at 1580 cm^{-1}. All other fibers also exhibit a disorder-induced line at 1360 cm^{-1} and an increased line width for the line at 1580 cm^{-1}. From top to bottom, the spectra were generated by the heat-treated CVD fiber, the as-grown CVD fiber, P 100, P 55, the heat-treated Celion 6000 fiber, and the FMI fiber. The curves drawn through the experimental points are Lorentzian fits to the data corresponding to the parameters reported in Table I. The resulting integrated intensities were used to generate the ratios I_{1360}/I_{1580}

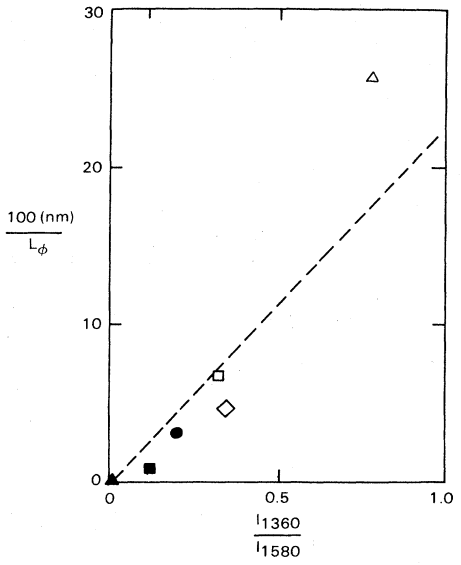

FIG. 5. Correlation between the defect-limited phonon mean free path L_ϕ deduced from the low-temperature thermal-conductivity data (represented on the ordinate axis as 100 nm/L_ϕ), and on the abscissa, the ratio I_{1360}/I_{1580} between the integrated intensities of the disorder-induced and the Raman allowed line at 1360 cm^{-1} and the allowed Raman line at 1580 cm^{-1}. The symbols used for the various samples are the same as in Fig. 2. The dashed line represents a similar correlation obtained in Ref. 3 between 100 nm/L_a and I_{1360}/I_{1580}, where L_a is the in-plane x-ray correlation length.

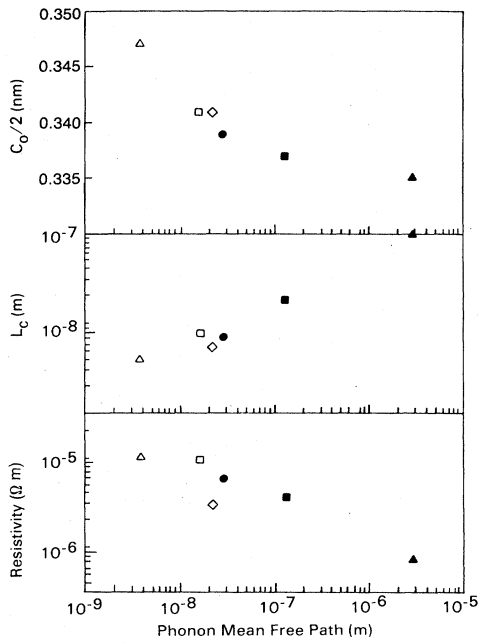

FIG. 6. Results of x-ray diffraction patterns and electrical resistivity plotted versus the phonon mean free path. The top frame shows the c-axis interplane distance on a linear ordinate; the middle frame has a logarithmic ordinate representing L_c, the c-axis correlation length as deduced from the line width of the ⟨002⟩ peak. In the bottom frame the room-temperature value of the electrical resistivity is plotted on a logarithmic ordinate. The abscissa is the defect-limited phonon mean free path L_ϕ. The symbols again identify the various samples, as described in Fig. 2.

data. A clear correlation is obtained, in spite of the fact that Raman scattering only probes less than 1000 Å into the fibers while the thermal conductivity is a bulk property, and the measurements were obtained on fibers prepared in three very different ways. However, the larger uncertainty in the Raman spectra obscures our data on the PAN-based fibers.

In Ref. 3, the intensity ratio I_{1360}/I_{1580} was related to the in-plane crystallite size L_a. Using only a diffractometer, we have been unable to generate reliable values for this quantity for all types of fibers without explicit use of a model for the morphology of the carbon samples being used. It seems to us that the phonon mean free path L_ϕ is a much more model-independent variable quantitatively describing the degree of in-plane order. In Fig. 5, we plotted, as a dashed line, the correlation between 100 nm/L_a and I_{1360}/I_{1580} as reported in Ref. 3. This figure shows good evidence that L_a and L_ϕ not only vary in similar ways with crystalline perfection, but also are of very comparable magnitude.

The lower frame of Fig. 6 shows a plot of the room-temperature electrical resistivity as a function of the phonon mean free path. The resistivity of the highly stretched and heat-treated PAN-based fiber FMI is significantly lower than that of the other fibers. The two upper frames of Fig. 6 illustrate how the x-ray data describing the c-axis interlayer spacing ($\frac{1}{2}c_0$) and coherence length (L_c) vary with the phonon mean free path L_ϕ which measures in-plane order. Although a correlation between these c-axis properties and L_ϕ is not *a priori* expected, it appears experimentally and confirms previous results.[22]

ACKNOWLEDGMENT

The authors gratefully acknowledge many useful discussions with Professor J.-P. Issi, Dr. G. Dresselhaus, Dr. C. P. Beetz, Jr., and Dr. G. G. Tibbetts who also provided the CVD fibers, and with Mr. C. Olk. The M.I.T. authors acknowledge support from DOE Grant No. DE-AC02-83ER45041

[1]L. Piraux, B. Nysten, A. Haquenne, J.-P. Issi, M. S. Dresselhaus, and M. Endo, Solid State Commun. **50**, 697 (1984).

[2]J. Heremans and C. P. Beetz, Phys. Rev. B **32**, 1981 (1985); also in Extended Abstracts of the 17th Carbon Conference, Lexington, Kentucky, 1985, p. 235 (unpublished).

[3]F. Tuinstra and J. L. Koenig, J. Compos. Mater. **4**, 492 (1970); J. Chem. Phys. **53**, 1126 (1970).

[4]P. Lespade, R. Al-Jishi, and M. S. Dresselhaus, Carbon **20**, 427 (1982).

[5]J. C. Bowman, J. A. Krumhansl, and J. T. Meers, *Industrial Carbon and Graphite* (Society of Chemical Industry, London, 1958).

[6]Union Carbide Technical Information Bulletin No. 465 235, and Product Information Thornel P 100-2 K, Union Carbide Corporation, Carbon Products Division, 120 S. Riverside Plaza, Chicago, IL (unpublished).

[7]B. Nysten, L. Piraux, and J.-P. Issi, J. Phys. D **18**, 1307 (1985).

[8]D. J. Radcliffe and H. M. Rosenberg, Cryogenics **22**, 245 (1979).

[9]M. W. Pilling, B. Yates, M. A. Black, and P. Tattersall, J. Mater. Sci. **14**, 1326 (1979).

[10]V. I. Volga, V. I. Frolov, and V. K. Usov, Inorg. Mater. **9**, 643 (1973).

[11]J. L. Hull, Z. Chiba, and P. Johnson, Extended Abstracts of the 14th Biennial Conference on Carbon, University Park, Pennsylvania (1979), p. 228 (unpublished).

[12]G. G. Tibbetts, Appl. Phys. Lett. **42**, 666 (1983).

[13]Celanese Corp., Advanced Engineering Components, 26 Main Street, Chatham, New Jersey.

[14]See, for example, U.S. Army Final Technical Report Contract No. DAAK 70-C-79-0209 (unpublished).

[15]B. D. Cullity, *Elements of X-ray Diffraction* (Addision-Wesley, Reading, Mass., 1956).

[16]W. Yetter, C. P. Beetz, Jr., and G. W. Budd, Extended Abstracts of the 17th Carbon Conference, Lexington, Kentucky, 1985, p. 291 (unpublished).

[17]L. S. Singer, U.S. Patent No. 4005183 (25 Jan. 1977); see also, for instance, S. Chwastiak, J. B. Barr, and R. Didchenko, Carbon **17**, 49 (1979).

[18]D. J. Johnson, Chem. Ind. **18**, 692 (1982).

[19]B. T. Kelly, *Physics of Graphite* (Applied Science, London, 1981).

[20]R. Perret and W. Ruland, J. Appl. Crystallogr. **3**, 525 (1970).

[21]T. C. Chieu, M. S. Dresselhaus, and M. Endo, Phys. Rev. B **26**, 5867 (1982).

[22]I. L. Spain: Phys. Chem. Carbon **16**, 119 (1978).